

# Characterization of intratumoral follicular helper T cells in follicular lymphoma: role in the survival of malignant B cells

Patricia Amé-Thomas<sup>1</sup>, Jérôme Le Priol<sup>1</sup>, Hans Yssel<sup>2</sup>, Gersende Caron<sup>1</sup>, Céline Pangault<sup>1</sup>, Rachel Jean<sup>1</sup>, Nadine Martin<sup>3,4</sup>, Teresa Marafioti<sup>5</sup>, Philippe Gaulard<sup>3,4</sup>, Thierry Lamy<sup>1</sup>, Thierry Fest<sup>1</sup>, Gilbert Semana<sup>1</sup>, Karin Tarte<sup>1\*</sup>

<sup>1</sup> Microenvironnement et cancer INSERM : U917, Université de Rennes 1, Biosit, EFS Bretagne, 2 avenue du Professeur Léon Bernard, 35043 Rennes Cedex, FR

<sup>2</sup> Cellules souches mésenchymateuses, environnement articulaire et immunothérapies de la polyarthrite rhumatoïde INSERM : U844, IFR3, Université Montpellier I, Hôpital Saint Eloi - Bâtiment INM 80 rue Augustin Fliche BP 74103 - 34091 Montpellier cedex 5, FR

<sup>3</sup> Institut Mondor de Recherche Biomédicale INSERM : U955, Université Paris XII - Paris Est Créteil Val-de-Marne, IFR10, 8 rue du général Sarrail 94010 Créteil, FR

<sup>4</sup> Service d'anatomie et cytologie pathologiques [Mondor] Assistance publique - Hôpitaux de Paris (AP-HP), Hôpital Henri Mondor, Université Paris XII - Paris Est Créteil Val-de-Marne, 51 Av Maréchal de Lattre de Tassigny, 94000 Créteil, FR

<sup>5</sup> Department of histopathology University College Hospital, London, GB

\* Correspondence should be addressed to: Karin Tarte <karin.tarte@univ-rennes1.fr >

## Abstract

Accumulating evidences indicate that the cellular and molecular microenvironment of follicular lymphoma (FL) plays a key role in both lymphomagenesis and patient outcome. Malignant FL B cells are found admixed to specific stromal and immune cell subsets, in particular CD4<sup>pos</sup> T cells displaying phenotypic features of follicular helper T cells (T<sub>FH</sub>). The goal of our study was to functionally characterize intratumoral CD4<sup>pos</sup> T cells. We showed that CXCR5<sup>hi</sup> ICOS<sup>hi</sup> CD4<sup>pos</sup> T cells sorted from FL biopsies comprise at least two separate cell populations with distinct genetic and functional features: i) CD25<sup>pos</sup> follicular regulatory T cells (T<sub>FR</sub>), and ii) CD25<sup>neg</sup> T<sub>FH</sub> displaying a FL-B cell supportive activity without regulatory functions. Furthermore, despite their strong similarities with tonsil-derived T<sub>FH</sub>, purified FL-derived T<sub>FH</sub> displayed a specific gene expression profile including an overexpression of several genes potentially involved directly or indirectly in lymphomagenesis, in particular *TNF*, *LTA*, *IL4*, or *CD40LG*. Interestingly, we further demonstrated that these two last signals efficiently rescued malignant B cells from spontaneous and Rituximab-induced apoptosis. Altogether, our study demonstrates that tumor-infiltrating CD4<sup>pos</sup> T cells are more heterogeneous than previously presumed, and underlines for the first time the crucial role of T<sub>FH</sub> in the complex set of cellular interactions within FL microenvironment.

**MESH Keywords** Antigens, CD4; immunology; B-Lymphocytes; pathology; Cell Survival; immunology; Flow Cytometry; Gene Expression Profiling; Humans; Immunohistochemistry; Immunophenotyping; Interleukin-2 Receptor alpha Subunit; immunology; Lymphoma, Follicular; genetics; immunology; pathology; Receptors, CXCR5; metabolism; Reverse Transcriptase Polymerase Chain Reaction; T-Lymphocytes, Helper-Inducer; immunology

**Author Keywords** follicular lymphoma; follicular helper T cells; follicular regulatory T cells

## INTRODUCTION

Follicular lymphoma (FL), the most frequent indolent non-Hodgkin lymphoma (NHL), results from the transformation of germinal center (GC) B cells (1). Besides a complex set of intrinsic genetic abnormalities, FL B cells retain, like their normal counterpart, a strong dependence on their molecular and cellular microenvironment. Indeed, malignant B cells are found admixed with specific stromal cell subsets (2) and CD4<sup>pos</sup> T cells (3), which form a specialized malignant cell niche within invaded lymphoid organs. Importantly, gene expression profile studies performed on whole tissue biopsies have revealed that the outcome of FL patients was not primarily predicted by the gene expression pattern of tumor B cells, but by gene signatures of non-malignant tumor infiltrating cells, with a favorable outcome related to T-cell restricted genes (4).

Several reports have confirmed that the nature and the localization of T cells within invaded lymph nodes (LN) could be used as prognostic biomarkers. Interestingly, the localization of CD4<sup>pos</sup> T cells within neoplastic follicles, unlike their absolute number, was consistently associated with poor survival and rapid transformation (5), suggesting that different CD4<sup>pos</sup> T cell subsets could display different functions in FL. Among them, regulatory T cells (Treg) are supposed to play a central role. Surprisingly, an increased number of FOXP3<sup>pos</sup> Treg has been first associated with improved overall survival (6). However, their follicular localization was thereafter associated with poor progression-free and overall survival, as well as a high risk of transformation (7). Furthermore, convincing functional studies revealed that natural and induced FL Treg were endowed with suppressive capacities towards infiltrating CD4<sup>pos</sup> effector T cells and CD8<sup>pos</sup> cytotoxic T cells (8–10). Overall, these data suggest that, like in solid tumors, Treg inhibit antitumor responses in FL. Other immunohistochemistry studies have focused on markers harbored by follicular helper T cells (T<sub>FH</sub>), the specialized subset of CD4<sup>pos</sup> T cells present within secondary lymphoid organs (SLO). T<sub>FH</sub> provide survival signals to antigen-selected GC B cells, and help them to

achieve class-switch recombination and differentiation into antibody-secreting plasma cells. Highly controversial findings were reported concerning the prognostic value of the number and localization of PD1<sup>pos</sup> and CD57<sup>pos</sup> T cells (5, 11–13). However, the phenotypic definition of T<sub>FH</sub> requires a combination of several markers thus limiting the impact of single marker-based immunohistochemistry studies. In addition, whereas we recently identified a T<sub>FH</sub>-dependent IL-4 centered pathway in FL, no functional study has been performed yet to explore the specific role of the T<sub>FH</sub> compartment on malignant FL B cells.

T<sub>FH</sub> are characterized by a strong expression of CXCR5 associated with a lack of CCR7 allowing their migration and retention into the CXCL13-rich light zone of GC. In addition, they express high levels of inducible costimulator (ICOS), CD200, PD-1, and produced IL-21 and CXCL13 (14). These features are essentially associated with the expression of the transcription factor BCL-6, the master regulator of T<sub>FH</sub> differentiation (15). Importantly, T<sub>FH</sub> subset has emerged as an independent CD4<sup>pos</sup> T helper lineage with distinct developmental program and effector functions. However, several recent reports revealed a higher plasticity within T helper lineages than previously anticipated. In particular, studies conducted in mice and humans demonstrated that T<sub>FH</sub> could secrete IFN- $\gamma$ , IL-4, and IL-17, the prototypic Th1, Th2, and Th17 cytokines (16–18).

Owing to the demonstration that, in both mice and human, CXCR5 and ICOS are two of the most relevant phenotypic T<sub>FH</sub> cell markers (19, 20), we aimed to fully characterize CXCR5<sup>hi</sup> ICOS<sup>hi</sup> CD4<sup>pos</sup> T cells infiltrating FL tumors. In addition, since i) human tonsil CD4<sup>pos</sup> CD57<sup>pos</sup> T<sub>FH</sub> have been described to exert regulatory functions *in vitro* (21), and ii) Treg could localize within malignant follicles in FL (7) whereas they are essentially found in the extrafollicular zones in reactive lymph nodes (22), we decided to explore the relationship between T<sub>FH</sub> and Treg in the FL context. We encompassed that the CXCR5<sup>hi</sup> ICOS<sup>hi</sup> CD4<sup>pos</sup> phenotypic definition merged two distinct functional T-cell populations in FL based on the expression of CD25: a CD25<sup>pos</sup> follicular Treg (T<sub>FR</sub>) subset and a CD25<sup>neg</sup> T<sub>FH</sub> subset. Finally, we demonstrated that FL-derived T<sub>FH</sub> displayed a gene expression pattern close but distinct from that of tonsil-derived T<sub>FH</sub> and exhibited a strong supportive activity on malignant FL B cells mediated in part by CD40L and IL-4.

## MATERIALS AND METHODS

### Cell samples

All tissues used for this study came from subjects recruited under institutional review board approval and informed consent process according to the Declaration of Helsinki. Samples were obtained from LN of patients with *de novo* FL, diffuse large B-cell lymphoma (DLBCL), or with reactive non-malignant diseases considered as normal counterpart, and from tonsils collected from children undergoing routine tonsillectomy. All FL LN showed a predominant follicular growth pattern and were classified into grades 1, 2, or 3a according to the WHO diagnostic criteria. Tissues were cut into pieces and flushed using syringes and needles. The CD4<sup>pos</sup> T cell enriched fraction was obtained as previously described (17). T<sub>FH</sub>, T<sub>FR</sub>, and nonT<sub>FH</sub> were sorted using a FACSAria (Becton Dickinson, San Diego, CA) as CD3<sup>pos</sup> CD4<sup>pos</sup> CXCR5<sup>hi</sup> ICOS<sup>hi</sup> CD25<sup>neg</sup>, CD3<sup>pos</sup> CD4<sup>pos</sup> CXCR5<sup>hi</sup> ICOS<sup>hi</sup> CD25<sup>pos</sup>, and CD3<sup>pos</sup> CD4<sup>pos</sup> CXCR5<sup>neg</sup> ICOS<sup>neg</sup> cells, respectively. Purity of each fraction was greater than 98%. Primary FL B cells were purified as previously described (23). Purity of CD19<sup>pos</sup> B cells was greater than 99%, and more than 95% of these cells expressed the appropriate tumor isotype light chain. Magnetic cell sorts using the StemSep CD4<sup>pos</sup> T Cell Enrichment Kit (Stemcell Technologies, Vancouver, Canada) and the CD25 Microbeads II (Miltenyi Biotech, Gladbach, Germany) were performed to isolate CD4<sup>pos</sup> CD25<sup>neg</sup> effector T cells from PBMC, and tonsil CD4<sup>pos</sup> CD25<sup>pos</sup> cells required for the sorting of CD4<sup>pos</sup> CD25<sup>hi</sup> CD127<sup>low</sup> Treg. Th1, Th2, and Th17 clones were obtained from biopsies taken from active inflammatory lesions of patients suffering from chronic inflammatory or auto-immune diseases, as previously described (24).

### Quantitative RT-PCR

Total RNA was extracted using RNeasy Kit (Qiagen, Valencia, CA). All samples used displayed an RNA integrity number of at least 9.4. cDNA was then generated using Superscript II reverse transcriptase (Invitrogen, Carlsbad, CA). For quantitative RT-PCR, we used assay-on-demand primers and probes (Table S1), and the Taqman Universal Master Mix from Invitrogen. Gene expression was measured using the ABI Prism 7000, or the ABI Prism 7900HT Sequence Detection System when predesigned TaqMan Array Micro Fluidic Cards were used. *B2M*, *CASC3*, and *I8S* was determined as appropriate internal standard genes (25). For each sample, the C<sub>T</sub> value for the gene of interest was determined, normalized to the geometric mean value of the 3 housekeeping genes, and compared to the value obtained from a pool of peripheral blood naive CD4<sup>pos</sup> T cells. A hierarchical clustering algorithm was used to group genes on the basis of similarity and data visualization was carried out with Cluster and Treeview (Eisen softwares, Stanford, CA). Supervised analyses included two approaches: 1) Significance Analysis of Microarrays (SAM) software, using 500 permutations, a fold change > 2 or < 0.5 and an false discovery rate < 3%; 2) Unpaired Mann-Whitney non-parametric test carried out with Partek<sup>®</sup> Genomics Suite software (Partek, Saint Louis, MO), and selection of gene with a *P*-value less than 0.05. Generated gene lists were then crossed to retain only overlapping genes. Principal Component Analysis (PCA) was conducted using Partek<sup>®</sup> Genomics Suite.

### Flow cytometry characterization

Monoclonal antibodies (mAbs) used are listed on Table S2 . Data were analyzed using Kaluza software (Beckman Coulter, Miami, FL). For IL-4 and IFN- $\gamma$  detection, total FL LN or tonsil cell suspensions were stimulated with 100 ng/mL of phorbol 12-myristate 13-acetate and 750 ng/mL of ionomycin for 6 hours in RPMI 10% fetal calf serum (FCS) at 37°C. Ten  $\mu$ g/mL of brefeldin A (BD Biosciences) were added for the last 4 hours of stimulation. The percentage of viable CD3<sup>pos</sup> T cells, nonT<sub>FH</sub>, and T<sub>FH</sub> producing IL-4 and IFN- $\gamma$  was determined by staining with live/dead fixable yellow dead cell stain kit (Invitrogen) and cell-subset gating mAbs before fixation and permeabilization using the Cytotfix/Cytoperm Fixation/Permeabilization Solution Kit (BD Biosciences) and incubation with anti IL-4 or anti-IFN- $\gamma$  mAbs.

### Immunohistochemistry studies

Immunohistochemistry was performed on deparaffinized tissue sections of FL LN, reactive LN with follicular hyperplasia, and tonsils using a standard indirect avidin-biotin immunoperoxidase method. Briefly, after appropriate antigen retrieval, sections were incubated with anti-human ICOS (provided by Dr T. Marafioti) and anti-human FOXP3 (clone 236A/E7 Abcam, Cambridge, UK) mAbs. Double immunostainings were performed as previously described (26 ). Images were captured with a Zeiss Axioskop2 microscope (Zeiss, Oberkochen, Germany) and Neofluar 100x/0.1 NA optical lenses (Zeiss). Photographs were taken with a DP70 Olympus camera (Olympus, Tokyo, Japan). Image acquisition was performed with Olympus DP Controller 2002, and images were processed with Adobe Photoshop v7.0 (Adobe Systems, San Jose, CA).

### B-cell anti-apoptotic assay

Purified FL malignant B cells were cultured in IMDM 10% FCS in round bottom 96-well plates alone or in presence of purified T-cell subsets (ratio 1:1). After 24 hours, cells were harvested and B-cell apoptosis was assessed on gated CD20<sup>pos</sup> CD4<sup>neg</sup> B cells using active caspase-3 PE apoptosis kit (Becton Dickinson), according to manufacturer's instructions. In addition, B-cell activation was evaluated in the same culture conditions after 40 hours of culture, by the ratio of the mean fluorescence intensity (RMFI) obtained with phycoerythrin-conjugated CD86 mAb and its isotype-matched negative control (Beckman Coulter).

### Suppression assay

Effector T cells were stained with 5 $\mu$ M of carboxyfluorescein diacetate succinimidyl ester (CFSE, Invitrogen) and resuspended in IMDM 10% AB human serum (HS), 0.2  $\mu$ g/mL anti-CD3 (Sanquin, Amsterdam, The Netherlands) and 0.1  $\mu$ g/mL anti-CD28 (Becton Dickinson) mAbs. Cultures were performed in round bottom 96-well culture plates, in the presence or not of T<sub>FH</sub>, nonT<sub>FH</sub>, Treg, or T<sub>FR</sub> (ratio of 1:1) for 5 days. CFSE<sup>pos</sup> TOPRO-3<sup>neg</sup> viable effector T cells were analyzed. Percentages of cells in each generation were identified using the ModFit software (Verity Software, Topsham, ME).

### Rituximab-induced cell death assay

Purified FL malignant B cells were plated in round bottom 96-well plates in IMDM 50% AB HS, and stimulated or not for 3 hours with 50 ng/mL CD40L, 35 ng/mL enhancer polyhistidine mAb, and 50 ng/mL IL-4 (RD Systems, Abingdon, UK) before 21 hours of culture in the presence or not of 25  $\mu$ g/mL anti-CD20 mAb Rituximab (Mabthera<sup>TM</sup>, Roche, Basel, Switzerland). The absolute number of TOPRO-3<sup>neg</sup> viable FL B cells was evaluated using Flowcount beads.

### Statistical analyses

Statistical analyses were performed with the GraphPad Prism software using non-parametric Kruskal-Wallis test, Wilcoxon test for matched pairs, or Mann Whitney U tests.

## RESULTS

### Phenotypic description of CXCR5<sup>hi</sup> ICOS<sup>hi</sup> CD4<sup>pos</sup> T cells in reactive and malignant secondary lymphoid organs

We first quantified by flow cytometry CXCR5<sup>hi</sup> ICOS<sup>hi</sup> CD4<sup>pos</sup> T cells in dissociated samples of reactive LN and tonsils, as well as in infiltrated LN from patients with FL and *de novo* DLBCL. As previously described (17 ), we found a similarly high proportion of T<sub>FH</sub> in tonsils (median: 30% [5–57]) and FL LN (median: 32% [10–57]). The percentage of CXCR5<sup>hi</sup> ICOS<sup>hi</sup> cells among CD4<sup>pos</sup> T cells was low in the majority of reactive LN, with the exception of few samples with major follicular hyperplasia, as evaluated by morphological analysis of tissue sections. Interestingly, T<sub>FH</sub> were not detected in the majority of DLBCL samples (median: 0.2% [0–20]) (Figure 1A ). PD-1 is another well-known T<sub>FH</sub> marker (14 ). Interestingly, whereas the percentage of T<sub>FH</sub> among CD4<sup>pos</sup> T cells was the same using both the CXCR5<sup>hi</sup> ICOS<sup>hi</sup> and the CXCR5<sup>hi</sup> PD-1<sup>hi</sup> definitions in tonsils, the percentage of CXCR5<sup>hi</sup> PD-1<sup>hi</sup> CD4<sup>pos</sup> T cells represented only 78.8  $\pm$  21% of that of CXCR5<sup>hi</sup> ICOS<sup>hi</sup> CD4<sup>pos</sup> T cells in FL, suggesting an additional level of heterogeneity within CXCR5<sup>hi</sup> ICOS<sup>hi</sup> CD4<sup>pos</sup> T-cell subset in this disease (Figure 1B ).

Because previous data suggested that Treg could be specifically recruited in follicles in FL context (9), we also decided to characterize more precisely this population. We evaluated the expression of CD25 and FOXP3 among CD4<sup>pos</sup> T cells within SLO. We revealed a higher frequency of FOXP3<sup>pos</sup> CD25<sup>pos</sup> Treg among CD4<sup>pos</sup> T cells in FL, compared to tonsils, reactive LN, and DLBCL samples (Figure 1C). Interestingly, we noticed that FL LN samples were particularly enriched for CD4<sup>pos</sup> T cells harbouring both CXCR5<sup>hi</sup> ICOS<sup>hi</sup> and FOXP3<sup>pos</sup> CD25<sup>pos</sup> phenotypes and were called thereafter follicular regulatory T cells (T<sub>FR</sub>) (Figure 2A). In order to evaluate if this phenotype was really associated to a follicular localization, double-immunostainings were performed on FL biopsies and confirmed the presence of numerous FOXP3<sup>pos</sup> cells co-expressing ICOS essentially within FL neoplastic follicles (Figure 3A). On the contrary, these cells were rare in GC of follicular hyperplasia, and were localized in the interfollicular areas or at the periphery of GC (Figure 3B), in accordance with their homogeneous low expression of CXCR5 in tonsils (Figure 2B). Finally, whereas no correlation was found between the proportions of total Treg and T<sub>FR</sub> in FL samples, we revealed a strong correlation between FL T<sub>FR</sub> and T<sub>FH</sub> contents (p=0.02) (Figure 2C).

Overall, we pointed out three CD4<sup>pos</sup> T-cell subsets in FL LN: classical CD4<sup>pos</sup> CXCR5<sup>hi</sup> ICOS<sup>hi</sup> CD25<sup>neg</sup> FOXP3<sup>neg</sup> T<sub>FH</sub>, classical CD4<sup>pos</sup> CXCR5<sup>neg</sup> ICOS<sup>neg</sup> CD25<sup>pos</sup> FOXP3<sup>pos</sup> Treg, and a new CD4<sup>pos</sup> CXCR5<sup>hi</sup> ICOS<sup>hi</sup> CD25<sup>pos</sup> FOXP3<sup>pos</sup> T<sub>FR</sub> compartment.

### Definition of CXCR5<sup>hi</sup> ICOS<sup>hi</sup> CD4<sup>pos</sup> T cells in FL LN

To further explore the complexity of follicular CD4<sup>pos</sup> T cells in FL, we compared by quantitative RT-PCR, the gene expression profile of *ex-vivo* sorted Treg, FL-derived T<sub>FR</sub>, and FL- and tonsil-derived T<sub>FH</sub>. We also included in our analysis Th1, Th2, and Th17 clones derived from chronically inflamed human tissues that were shown to be highly representative of T-cell polarization in humans (24, 27). This study involved 45 genes that play a pivotal role in CD4<sup>pos</sup> T cell differentiation, localization and effector functions (Table S1). The results of a PCA analysis revealed that FL and tonsil-derived T<sub>FH</sub> shared a very close gene expression signature, compared to Th1, Th2, Th17, Treg, and FL T<sub>FR</sub> (Figure 4A). In addition, an unsupervised clustering analysis allowed to properly classify FL- and tonsil-derived T<sub>FH</sub>, and ordered FL T<sub>FR</sub> closer to Treg than T<sub>FH</sub> (Figure 4B). More precisely, we then focused on the expression of the master regulators of each helper T-cell lineage, *i.e.* *TBX21*, *GATA3*, *RORC*, *FOXP3*, and *BCL6* involved and over-expressed during the Th1, Th2, Th17, Treg and T<sub>FH</sub> cell differentiation, respectively. We confirmed that FL and tonsil-derived T<sub>FH</sub> expressed lower to undetectable levels of *TBX21*, *GATA3*, and *RORC*, compared to Th1, Th2, and Th17. In addition, T<sub>FR</sub> and Treg exhibited a similarly high level of *FOXP3*, unlike FL and tonsil-derived T<sub>FH</sub>. FL- and tonsil-derived T<sub>FH</sub> strongly expressed *BCL6* and were devoid of *PRDM1* expression, whereas FL T<sub>FR</sub> strongly expressed *PRDM1* (Figure 4C). Overall, when focusing on T-helper differentiation genes, our data highlighted that FL-derived T<sub>FH</sub> and T<sub>FR</sub> shared a highly similar gene expression pattern with tonsil T<sub>FH</sub> and Treg, respectively. However, T<sub>FR</sub> retained a higher *BCL6* expression than classical Treg and the amount of *PDCDI* (encoding PD1) transcripts was intermediate in T<sub>FR</sub>, as compared to T<sub>FH</sub> and Treg. Finally, FL T<sub>FH</sub> displayed the classical PD-1<sup>hi</sup> CD200<sup>hi</sup> CD127<sup>low</sup> CD57<sup>pos/neg</sup> phenotype, previously ascribed to normal LN T<sub>FH</sub>, whereas FL T<sub>FR</sub> could be defined as PD-1<sup>dim</sup> CD200<sup>dim</sup> CD127<sup>low</sup> CD57<sup>pos/neg</sup> CD4<sup>pos</sup> T cells (Figure S1). These data were helpful to reconcile the discrepancy, within FL biopsies, between the percentages of CXCR5<sup>hi</sup> CD4<sup>pos</sup> T cells co-expressing high levels of ICOS (comprising T<sub>FH</sub> and T<sub>FR</sub>) *versus* high levels of PD-1 (comprising T<sub>FH</sub> only) (Figure 1B) and confirmed that T<sub>FR</sub> constitute a specific new cell subset distinct from both T<sub>FH</sub> and Treg.

### Functional characterization of CXCR5<sup>hi</sup> ICOS<sup>hi</sup> CD4<sup>pos</sup> T cells in FL LN

T<sub>FH</sub> are defined by their capacity to support antigen-specific B-cell response by providing survival, activation, differentiation, and class switch recombination signals to normal B cells (14). We first explored malignant B cell activation and survival in coculture with CD4<sup>pos</sup> T-cell subsets. FL B cells upregulated the expression of the CD86 activation antigen when cultured with autologous T<sub>FH</sub>, and not with CXCR5<sup>neg</sup> ICOS<sup>neg</sup> CD4<sup>pos</sup> nonT<sub>FH</sub> (Figure 5A). Similarly, T<sub>FH</sub>, unlike both nonT<sub>FH</sub> and T<sub>FR</sub>, were able to rescue autologous malignant B cells from spontaneous apoptosis *in vitro* (Figure 5B).

Furthermore, functional studies revealed that whereas T<sub>FR</sub> did not display a malignant B-cell supportive effect, they exerted a strong regulatory potential, as demonstrated by their capacity to inhibit CD4<sup>pos</sup> CD25<sup>neg</sup> effector T-cell proliferation as efficiently as tonsil Treg used as a control (Figures 5B–C). In the same experiment, paired FL T<sub>FH</sub> displayed no regulatory properties (Figure 5C). These results convincingly demonstrated that T<sub>FR</sub> could be considered as *bona fide* regulatory T cells expressing the GC specific receptor CXCR5.

In conclusion, our functional results convincingly demonstrated that, in FL, the CXCR5<sup>hi</sup> ICOS<sup>hi</sup> CD4<sup>pos</sup> T-cell definition included both functional CXCR5<sup>hi</sup> ICOS<sup>hi</sup> CD25<sup>neg</sup> CD4<sup>pos</sup> T<sub>FH</sub> with anti-apoptotic activity on autologous malignant B cells, and CXCR5<sup>hi</sup> ICOS<sup>hi</sup> CD25<sup>pos</sup> CD4<sup>pos</sup> functional Treg.

### CD40L/CD40 and IL-4/IL-4Rα are involved in FL B cell supportive activity of autologous T<sub>FH</sub>

Despite the similarities between T<sub>FH</sub> obtained from FL LN and tonsils, we next tried to unravel the specificity of T<sub>FH</sub> in the malignant context. In fact, the unsupervised clustering analysis described above (Figure 4B) revealed some discrepancies between these two

populations. Statistical analysis using combined SAM and Mann-Whitney U-test highlighted a significant differential expression of 10 genes, including 8 genes upregulated in FL-derived T<sub>FH</sub> (Table 1 ). We focused our attention on 3 of them: the B-cell activating cell surface molecule *CD40LG* , and the prototypic Th1 and Th2 cytokines, *IFNG* and *IL4* , previously reported as secreted by murine and human T<sub>FH</sub> (17 , 28 , 29 ). We confirmed on a more important set of samples the significant over-expression of *CD40LG* and *IL4* in T<sub>FH</sub> sorted from FL-LN, compared to those isolated from tonsils (Figure 6A ). In addition, we found by flow cytometry that FL LN contained a higher frequency of IFN- $\gamma$  secreting T cells than tonsils (median: 19.3% [14–32] and 10.8% [8–18] for FL LN and tonsils, respectively,  $p < 0.05$ ), in particular in the T<sub>FH</sub> compartment (median 8.3% [6–22] and 4.5% [3–10], respectively,  $p < 0.05$ ) (Figure 6B ). Similarly, the frequency of T cells secreting IL-4 was also more important in FL LN (median 12.7% [7–15]), as compared to tonsils (median 1.2% [1–3],  $p < 0.01$ ), and this cytokine was predominantly produced by the T<sub>FH</sub> subset (Figure 6C ). Taken together, these results prompted us to evaluate the role of CD40L and IL-4, two molecules implicated in normal B-cell growth, in the supportive effect of FL T<sub>FH</sub> .

In order to answer this question, we first cultured FL LN samples in the presence of anti-CD40L and/or anti-IL-4R $\alpha$  neutralizing mAbs, and evaluated the survival of malignant FL B cells. We were able to detect a slight but significant inhibition of malignant B-cell survival in the presence of each specific neutralizing antibody. Indeed, anti-CD40L and anti-IL-4R $\alpha$  mAbs inhibited FL B cell survival by 11.5% [5.8–16.3] and 10.4% [1.6–11.5], respectively (n=4, data not shown). In order to better underline the direct anti-apoptotic activity of CD40L and IL-4 on FL B cells, we evaluated their impact on the survival of purified FL B cells, in the presence of the specific anti-CD20 mAb Rituximab, commonly used in the treatment of FL patients. These experiments were performed in the presence of human serum with an undamaged complement activity in order to evaluate the Rituximab-mediated complement-dependent cytotoxicity. Malignant B cells displayed a heterogeneous response to Rituximab cytotoxicity (median survival: 34%, [19–85]), as previously described (30 ). Nevertheless, whereas CD40L+IL-4 did not increase spontaneous FL B cell survival during short term culture, we observed a significant but highly variable decrease (median: 45%, [3–100], n=9) of Rituximab-dependent cytotoxicity in the presence of CD40L+IL-4 (Figure 6D ). Overall, these results demonstrated that CD40L and IL-4, which are both overexpressed by FL-derived T<sub>FH</sub> , contributed to FL B-cell survival.

## DISCUSSION

FL B cells are characterized by chromosomal aberrations, a strong dependence on BCR signaling, and a bidirectional and dynamic crosstalk with both stromal and hematopoietic microenvironment within follicular malignant niche. Several studies using gene expression profile or immunohistochemistry approaches have depicted the importance of CD4<sup>pos</sup> T cells, depending on their number, activation status, and localization within malignant follicles (5 , 12 ). To date, in FL, only few functional studies have been performed essentially focused on Treg. These data prompted us to better characterize follicular CD4<sup>pos</sup> T cells.

The primary goal of our study was to precisely define T<sub>FH</sub> in FL samples. We identified a high proportion of CXCR5<sup>hi</sup> ICOS<sup>hi</sup> CD4<sup>pos</sup> T<sub>FH</sub> in tonsils and reactive LN with a major follicular hyperplasia, correlated to the frequency of GC CD10<sup>pos</sup> B cells (data not shown), suggesting that T<sub>FH</sub> cells might be related to the level and/or duration of follicular activation. LN obtained from FL and *de novo* DLBCL, the two most frequent NHL, showed adverse proportions of CXCR5<sup>hi</sup> ICOS<sup>hi</sup> cells among CD4<sup>pos</sup> T cells, unrelated to the cancer-associated activation context. This observation reinforces the notion that FL cells might require stronger interactions with surrounding cells than DLBCL cells. Indeed, despite the influence of immune cell infiltration on DLBCL biology (31 ), clinical behaviour is primarily predicted by tumor cell molecular signatures in aggressive lymphomas (32 ), whereas FL patient outcome, including overall survival and risk of transformation, is essentially related to the gene signature of non-malignant infiltrating cells (4 , 33 ). It will be interesting to evaluate the predictive value of T<sub>FH</sub> cell infiltration in a large cohort of homogeneously treated FL patients.

Importantly, we demonstrated that CXCR5<sup>hi</sup> ICOS<sup>hi</sup> CD4<sup>pos</sup> T cells from FL LN comprised two distinct functional subpopulations, based on the expression of CD25 and FOXP3: *bona fide* CD25<sup>pos</sup> Foxp3<sup>pos</sup> Treg called T<sub>FR</sub> , and CD25<sup>neg</sup>FOXP3<sup>neg</sup> T<sub>FH</sub> . Natural Treg expressing ICOS have already been described in healthy donors (22 ). In melanoma, accumulating Treg expressing high levels of ICOS have been reported among tumor-infiltrating T cells. This ICOS<sup>hi</sup> Treg subset displayed strong suppressive functions, and induced the activation of IL-4-secreting T cells (34 ). In addition, we demonstrated the presence of these FL T<sub>FR</sub> within neoplastic follicles, in accordance with their expression of CXCR5. The specific homing of Treg within neoplastic GC could result from two complementary processes: their specific recruitment, or their local induction/expansion. Interestingly, CCL22 secreted by FL B cells has been described as involved in the recruitment of Treg (9 ), and previous data reported that malignant B cells contributed to Treg differentiation (35 , 36 ). Importantly, two recent papers identify in mice a subset of CXCR5<sup>hi</sup> PD1<sup>hi</sup> Foxp3<sup>pos</sup> suppressive T cells that localize to the GC, coexpress *BCL6* and *PRDM1*, and arise from thymic-derived Foxp3<sup>pos</sup> precursors (37 , 38 ). They called them T<sub>FR</sub> cells. Our study provides strong evidence that this new T-cell population actually exists in human and is expanded during lymphomagenesis.

Here, we reported a strong correlation between T<sub>FR</sub> and T<sub>FH</sub> proportions, suggesting that CXCL13 secreted by T<sub>FH</sub> could contribute to the recruitment of CXCR5-expressing T<sub>FR</sub> within neoplastic follicles. In agreement, *CXCL13* was similarly highly expressed by tonsil and FL T<sub>FH</sub> (data not shown). Of note, no correlation between expression of *CXCL13* and *FOXP3* within FL microenvironment (data not

shown), or between the proportion of  $T_{FH}$  and total Treg have been found, reinforcing the specific relationship between  $T_{FH}$  and  $T_{FR}$ . Importantly, a recent report revealed the poor prognosis value of the follicular infiltration of FOXP3<sup>pos</sup> cells in FL biopsies (7). This may suggest that the  $T_{FR}$  subset plays an important role in FL pathogenesis through the inhibition of anti-tumor immune response. However, the low representation of  $T_{FR}$  in the FL microenvironment (median: 3% among CD4<sup>pos</sup> T cells) hampered us to perform more detailed functional investigations on this subset.

Beside this  $T_{FR}$  subpopulation, we demonstrated the presence of CXCR5<sup>hi</sup> ICOS<sup>hi</sup> CD25<sup>neg</sup> CD4<sup>pos</sup> T cells sustaining FL B cell survival and activation, and therefore matching the functional definition of  $T_{FH}$ . In addition, this subset brought all the phenotypic features of human tonsil  $T_{FH}$ . We were able to show that FL  $T_{FH}$ , like tonsil  $T_{FH}$ , expressed less *TBX21*, *GATA3*, *RORC*, and *FOXP3* than Th1, Th2, Th17 clones, and natural Treg, and a higher *BCL6/PRDM1* ratio. FL and tonsil  $T_{FH}$  also expressed similar levels of *IL21*, and *BTLA*. Importantly, no regulatory function was associated to CXCR5<sup>hi</sup> ICOS<sup>hi</sup> FL  $T_{FH}$ , contrary to previous data obtained with tonsil CD57<sup>pos</sup>  $T_{FH}$  (21). This apparent discrepancy may result from the different phenotypic definitions of  $T_{FH}$ . It has been demonstrated that CD57, unlike the CXCR5/ICOS combination, is not an appropriate marker of functional  $T_{FH}$  (20). In addition, we shown here that it could be more appropriate to define  $T_{FH}$  among CD4<sup>pos</sup> CD25<sup>neg</sup> T cells, as previously hypothesized (39), in order to reduce the potential contamination by Treg.

A more detailed analysis on selected genes revealed discrepancies between tonsil and FL  $T_{FH}$ . In particular, we demonstrated that FL-derived  $T_{FH}$  expressed more *IFNG*, *TNF*, and *LTA* than tonsil-derived  $T_{FH}$ . In a previous work, we reported an increased expression of these 3 genes in the entire microenvironment of FL B cells compared to normal tissues; and owing to the correlation between *IFNG*, *GRZA*, *GRZB*, and *CD8A* expression, we suggested the implication of cytotoxic cells in this secretion (23). Here, we demonstrated by quantitative RT-PCR experiments and flow cytometry strategies that  $T_{FH}$  were also involved in this overexpression of IFN- $\gamma$ . Of note, this secretion of IFN- $\gamma$ , TNF- $\alpha$  and LT- $\alpha$  by  $T_{FH}$  may have an influence on the FL B cell supportive effect of stromal cells, as described previously (23, 40). In addition, these inflammatory cytokines could also stimulate macrophages, which were shown to have an adverse effect on the outcome of FL patients (41, 42). We also observed an increased expression of the transcription factor aryl hydrocarbon receptor (AhR) in FL  $T_{FH}$ , compared to tonsil  $T_{FH}$ . AhR have been reported to regulate Th17, to induce the differentiation of Treg, and to enhance *CYP1A1*, *IL10*, or *IL22* expression (43–45). In the present study, gene expression data did not reveal an increased expression of these 3 genes in FL  $T_{FH}$ . However, it has also been reported that AhR could physically interact with c-Maf (43, 46), the transcription factor that specifically promotes IL-4 synthesis in Th2 cells. These two transcription factors could have a key role in the development and the functionality of IL-4-producing  $T_{FH}$  in FL context.

Finally, FL  $T_{FH}$  showed an increased expression of three B-cell growth factors, *i.e.* *IL2*, *IL4* and *CD40LG*, compared to tonsil  $T_{FH}$ . Flow cytometry analyses revealed a higher proportion of IL-4 secreting cells within FL  $T_{FH}$ . The CD40/CD40L pathway is central to multiple steps of B-cell survival, activation, and differentiation. The growth activity of CD40L has already been demonstrated on neoplastic mature B cells (23) and IL-4 exerts an antiapoptotic activity on normal B cells (47, 48). Nevertheless, a dual role for IL-4 was demonstrated on DLBCL malignant cells, with an increased sensitivity of GCB-like DLBCL to doxorubicin and Rituximab, whereas IL-4 protected ABC-like DLBCL from drug-induced apoptosis (49). In addition, a previous report demonstrated that IL-4 slightly and irregularly enhanced the proliferation of FL B cells *in vitro* (50). In our study, we highlighted a strong anti-apoptotic activity of CD40L and IL-4 on FL B cells treated *in vitro* with Rituximab. Interestingly, this anti-apoptotic effect was inversely correlated to the sensitivity of malignant FL B cells to Rituximab. Of note, beside its survival potential, IL-4 was also able to drive macrophages toward a TAM phenotype endowed with tumor invasion, immunoregulatory and pro-angiogenic properties (51).

In summary, our results depict new facets of the complex cellular interactions in FL and highlight the important supportive role of  $T_{FH}$  in the tumor microenvironment of FL malignant B cells. Targeting  $T_{FH}$  and their survival factors in combination with direct antitumor agents might be a promising strategy to provide new therapeutic schemes for FL patients.

## Acknowledgements:

This work was supported by research fundings from the Association pour la recherche sur le cancer (ARC AO 2007), the Institut National du Cancer (INCa translationnel 2010; PLBIO-10-195), and the Association pour le Développement de l'Héματο-Oncologie (ADHO). JLP was supported by a PhD studentship from the Association Leucémie Espoir. The authors are indebted to the Centre de Ressources Biologiques (CRB)-Santé of Rennes hospital for its support in the processing of biological samples, the Institut Fédératif de Recherche (IFR) 140 of Rennes for cell sorting core facility, and Christophe Raux for providing tonsil samples.

## Footnotes:

\* P.A.-T. and J.L.P. contributed equally to this work

**CONFLICT OF INTEREST** The authors declare no conflict of interest.

Supplementary Information accompanies the paper on the Leukemia website (<http://www.nature.com/leu>)

## References:

- 1 . Shaffer AL , Rosenwald A , Staudt LM . Lymphoid malignancies: the dark side of B-cell differentiation . *Nat Rev Immunol* . 2002 ; Dec 2 : (12 ) 920 - 932
- 2 . Thomazy VA , Vega F , Medeiros LJ , Davies PJ , Jones D . Phenotypic modulation of the stromal reticular network in normal and neoplastic lymph nodes: tissue transglutaminase reveals coordinate regulation of multiple cell types . *Am J Pathol* . 2003 ; Jul 163 : (1 ) 165 - 174
- 3 . Carbone A , Ghoghini A , Gruss HJ , Pinto A . CD40 ligand is constitutively expressed in a subset of T cell lymphomas and on the microenvironmental reactive T cells of follicular lymphomas and Hodgkin's disease . *Am J Pathol* . 1995 ; Oct 147 : (4 ) 912 - 922
- 4 . Dave SS , Wright G , Tan B , Rosenwald A , Gascoyne RD , Chan WC . Prediction of survival in follicular lymphoma based on molecular features of tumor-infiltrating immune cells . *N Engl J Med* . 2004 ; Nov 18 351 : (21 ) 2159 - 2169
- 5 . Glas AM , Knoops L , Delahaye L , Kersten MJ , Kibbelaar RE , Wessels LA . Gene-expression and immunohistochemical study of specific T-cell subsets and accessory cell types in the transformation and prognosis of follicular lymphoma . *J Clin Oncol* . 2007 ; Feb 1 25 : (4 ) 390 - 398
- 6 . Carreras J , Lopez-Guillermo A , Fox BC , Colomo L , Martinez A , Roncador G . High numbers of tumor-infiltrating FOXP3-positive regulatory T cells are associated with improved overall survival in follicular lymphoma . *Blood* . 2006 ; Nov 1 108 : (9 ) 2957 - 2964
- 7 . Farinha P , Al-Tourah A , Gill K , Klasa R , Connors JM , Gascoyne RD . The architectural pattern of FOXP3-positive T cells in follicular lymphoma is an independent predictor of survival and histologic transformation . *Blood* . 2010 ; Jan 14 115 : (2 ) 289 - 295
- 8 . Yang ZZ , Grote DM , Ziesmer SC , Manske MK , Witzig TE , Novak AJ . Soluble IL-2R{alpha} facilitates IL-2-mediated immune responses and predicts reduced survival in follicular B-cell non-Hodgkin lymphoma . *Blood* . 2011 ; in press
- 9 . Yang ZZ , Novak AJ , Stenson MJ , Witzig TE , Ansell SM . Intratumoral CD4+CD25+ regulatory T-cell-mediated suppression of infiltrating CD4+ T cells in B-cell non-Hodgkin lymphoma . *Blood* . 2006 ; May 1 107 : (9 ) 3639 - 3646
- 10 . Yang ZZ , Novak AJ , Ziesmer SC , Witzig TE , Ansell SM . Attenuation of CD8(+) T-cell function by CD4(+)CD25(+) regulatory T cells in B-cell non-Hodgkin's lymphoma . *Cancer Res* . 2006 ; Oct 15 66 : (20 ) 10145 - 10152
- 11 . Alvaro T , Lejeune M , Salvado MT , Lopez C , Jaen J , Bosch R . Immunohistochemical patterns of reactive microenvironment are associated with clinicobiologic behavior in follicular lymphoma patients . *J Clin Oncol* . 2006 ; Dec 1 24 : (34 ) 5350 - 5357
- 12 . Carreras J , Lopez-Guillermo A , Roncador G , Villamor N , Colomo L , Martinez A . High numbers of tumor-infiltrating programmed cell death 1-positive regulatory lymphocytes are associated with improved overall survival in follicular lymphoma . *J Clin Oncol* . 2009 ; Mar 20 27 : (9 ) 1470 - 1476
- 13 . Richentollar BG , Pohlman B , Elson P , Hsi ED . Follicular programmed death 1-positive lymphocytes in the tumor microenvironment are an independent prognostic factor in follicular lymphoma . *Hum Pathol* . 2011 ; Apr 42 : (4 ) 552 - 557
- 14 . Crotty S . Follicular Helper CD4 T Cells (TFH) . *Annu Rev Immunol* . 2011 ; Apr 23 29 : 621 - 663
- 15 . Johnston RJ , Poholek AC , DiToro D , Yusuf I , Eto D , Barnett B . Bcl6 and Blimp-1 are reciprocal and antagonistic regulators of T follicular helper cell differentiation . *Science* . 2009 ; Aug 21 325 : (5943 ) 1006 - 1010
- 16 . Ma CS , Suryani S , Avery DT , Chan A , Nanan R , Santner-Nanan B . Early commitment of naive human CD4(+) T cells to the T follicular helper (TFH) cell lineage is induced by IL-12 . *Immunol Cell Biol* . 2009 ; Nov-Dec 87 : (8 ) 590 - 600
- 17 . Pangault C , Ame-Thomas P , Ruminy P , Rossille D , Caron G , Baia M . Follicular lymphoma cell niche: identification of a preeminent IL-4-dependent TFH-B cell axis . *Leukemia* . 2010 ; Dec 24 : (12 ) 2080 - 2089
- 18 . Bauquet AT , Jin H , Paterson AM , Mitsdoerffer M , Ho IC , Sharpe AH . The costimulatory molecule ICOS regulates the expression of c-Maf and IL-21 in the development of follicular T helper cells and TH-17 cells . *Nat Immunol* . 2009 ; Feb 10 : (2 ) 167 - 175
- 19 . Akiba H , Takeda K , Kojima Y , Usui Y , Harada N , Yamazaki T . The role of ICOS in the CXCR5+ follicular B helper T cell maintenance in vivo . *J Immunol* . 2005 ; Aug 15 175 : (4 ) 2340 - 2348
- 20 . Rasheed AU , Rahn HP , Sallusto F , Lipp M , Muller G . Follicular B helper T cell activity is confined to CXCR5(hi)ICOS(hi) CD4 T cells and is independent of CD57 expression . *Eur J Immunol* . 2006 ; Jul 36 : (7 ) 1892 - 1903
- 21 . Marinova E , Han S , Zheng B . Germinal center helper T cells are dual functional regulatory cells with suppressive activity to conventional CD4+ T cells . *J Immunol* . 2007 ; Apr 15 178 : (8 ) 5010 - 5017
- 22 . Ito T , Hanabuchi S , Wang YH , Park WR , Arima K , Bover L . Two functional subsets of FOXP3+ regulatory T cells in human thymus and periphery . *Immunity* . 2008 ; Jun 28 : (6 ) 870 - 880
- 23 . Maby-El Hajjami H , Ame-Thomas P , Pangault C , Tribut O , DeVos J , Jean R . Functional alteration of the lymphoma stromal cell niche by the cytokine context: role of indoleamine-2,3 dioxygenase . *Cancer Res* . 2009 ; Apr 1 69 : (7 ) 3228 - 3237
- 24 . Pene J , Chevalier S , Preisser L , Venereau E , Guilleux MH , Ghannam S . Chronically inflamed human tissues are infiltrated by highly differentiated Th17 lymphocytes . *J Immunol* . 2008 ; Jun 1 180 : (11 ) 7423 - 7430
- 25 . Hamalainen HK , Tubman JC , Vikman S , Kyrola T , Ylikoski E , Warrington JA . Identification and validation of endogenous reference genes for expression profiling of T helper cell differentiation by quantitative real-time RT-PCR . *Anal Biochem* . 2001 ; Dec 1 299 : (1 ) 63 - 70
- 26 . Bruneau J , Canioni D , Renand A , Marafioti T , Paterson JC , Martin-Garcia N . Regulatory T-cell depletion in angioimmunoblastic T-cell lymphoma . *Am J Pathol* . 2010 ; Aug 177 : (2 ) 570 - 574
- 27 . Yssel H , De Vries JE , Koken M , Van Blitterswijk W , Spits H . Serum-free medium for generation and propagation of functional human cytotoxic and helper T cell clones . *J Immunol Methods* . 1984 ; Aug 3 72 : (1 ) 219 - 227
- 28 . Deenick EK , Chan A , Ma CS , Gatto D , Schwartzberg PL , Brink R . Follicular helper T cell differentiation requires continuous antigen presentation that is independent of unique B cell signaling . *Immunity* . 2010 ; Aug 27 33 : (2 ) 241 - 253
- 29 . Reinhardt RL , Liang HE , Locksley RM . Cytokine-secreting follicular T cells shape the antibody repertoire . *Nat Immunol* . 2009 ; Apr 10 : (4 ) 385 - 393
- 30 . Manches O , Lui G , Chaperot L , Gressin R , Molens JP , Jacob MC . In vitro mechanisms of action of rituximab on primary non-Hodgkin lymphomas . *Blood* . 2003 ; Feb 1 101 : (3 ) 949 - 954
- 31 . Monti S , Savage KJ , Kutok JL , Feuerhake F , Kurtin P , Mihm M . Molecular profiling of diffuse large B-cell lymphoma identifies robust subtypes including one characterized by host inflammatory response . *Blood* . 2005 ; Mar 1 105 : (5 ) 1851 - 1861
- 32 . Alizadeh AA , Eisen MB , Davis RE , Ma C , Lossos IS , Rosenwald A . Distinct types of diffuse large B-cell lymphoma identified by gene expression profiling . *Nature* . 2000 ; Feb 3 403 : (6769 ) 503 - 511
- 33 . de Jong D , de Boer JP . Predicting transformation in follicular lymphoma . *Leuk Lymphoma* . 2009 ; Sep 50 : (9 ) 1406 - 1411
- 34 . Strauss L , Bergmann C , Szczepanski MJ , Lang S , Kirkwood JM , Whiteside TL . Expression of ICOS on human melanoma-infiltrating CD4+CD25highFoxp3+ T regulatory cells: implications and impact on tumor-mediated immune suppression . *J Immunol* . 2008 ; Mar 1 180 : (5 ) 2967 - 2980
- 35 . Yang ZZ , Novak AJ , Ziesmer SC , Witzig TE , Ansell SM . CD70+ non-Hodgkin lymphoma B cells induce Foxp3 expression and regulatory function in intratumoral CD4+CD25 T cells . *Blood* . 2007 ; Oct 1 110 : (7 ) 2537 - 2544
- 36 . Yang ZZ , Novak AJ , Ziesmer SC , Witzig TE , Ansell SM . Malignant B cells skew the balance of regulatory T cells and TH17 cells in B-cell non-Hodgkin's lymphoma . *Cancer Res* . 2009 ; Jul 1 69 : (13 ) 5522 - 5530
- 37 . Linterman MA , Pierson W , Lee SK , Kallies A , Kawamoto S , Rayner TF . Foxp3(+) follicular regulatory T cells control the germinal center response . *Nat Med* . 2011 ; 17 : (8 ) 975 - 982
- 38 . Chung Y , Tanaka S , Chu F , Nurieva RI , Martinez GJ , Rawal S . Follicular regulatory T cells expressing Foxp3 and Bcl-6 suppress germinal center reactions . *Nat Med* . 2011 ; 17 : (8 ) 983 - 988
- 39 . Lim HW , Kim CH . Loss of IL-7 receptor alpha on CD4+ T cells defines terminally differentiated B cell-helping effector T cells in a B cell-rich lymphoid tissue . *J Immunol* . 2007 ; Dec 1 179 : (11 ) 7448 - 7456

- 40 . Ame-Thomas P , Maby-El Hajjami H , Monvoisin C , Jean R , Monnier D , Caulet-Maugendre S . Human mesenchymal stem cells isolated from bone marrow and lymphoid organs support tumor B-cell growth: role of stromal cells in follicular lymphoma pathogenesis . *Blood* . 2007 ; Jan 15 109 : ( 2 ) 693 - 702
- 41 . Byers RJ , Sakhinia E , Joseph P , Glennie C , Hoyland JA , Menasce LP . Clinical quantitation of immune signature in follicular lymphoma by RT-PCR-based gene expression profiling . *Blood* . 2008 ; May 1 111 : ( 9 ) 4764 - 4770
- 42 . Clear AJ , Lee AM , Calaminici M , Ramsay AG , Morris KJ , Hallam S . Increased angiogenic sprouting in poor prognosis FL is associated with elevated numbers of CD163+ macrophages within the immediate sprouting microenvironment . *Blood* . 2010 ; Jun 17 115 : ( 24 ) 5053 - 5056
- 43 . Gandhi R , Kumar D , Burns EJ , Nadeau M , Dake B , Laroni A . Activation of the aryl hydrocarbon receptor induces human type 1 regulatory T cell-like and Foxp3(+) regulatory T cells . *Nat Immunol* . 2010 ; Sep 11 : ( 9 ) 846 - 853
- 44 . Quintana FJ , Basso AS , Iglesias AH , Korn T , Farez MF , Bettelli E . Control of T(reg) and T(H)17 cell differentiation by the aryl hydrocarbon receptor . *Nature* . 2008 ; May 1 453 : ( 7191 ) 65 - 71
- 45 . Ramirez JM , Brembilla NC , Sorg O , Chicheportiche R , Matthes T , Dayer JM . Activation of the aryl hydrocarbon receptor reveals distinct requirements for IL-22 and IL-17 production by human T helper cells . *Eur J Immunol* . 2010 ; Sep 40 : ( 9 ) 2450 - 2459
- 46 . Apetoh L , Quintana FJ , Pot C , Joller N , Xiao S , Kumar D . The aryl hydrocarbon receptor interacts with c-Maf to promote the differentiation of type 1 regulatory T cells induced by IL-27 . *Nat Immunol* . 2010 ; Sep 11 : ( 9 ) 854 - 861
- 47 . Illera VA , Perandones CE , Stunz LL , Mower DA Jr , Ashman RF . Apoptosis in splenic B lymphocytes. Regulation by protein kinase C and IL-4 . *J Immunol* . 1993 ; Sep 15 151 : ( 6 ) 2965 - 2973
- 48 . Wurster AL , Rodgers VL , White MF , Rothstein TL , Grusby MJ . Interleukin-4-mediated protection of primary B cells from apoptosis through Stat6-dependent up-regulation of Bcl-xL . *J Biol Chem* . 2002 ; Jul 26 277 : ( 30 ) 27169 - 27175
- 49 . Sarosiek KA , Nechushtan H , Lu X , Rosenblatt JD , Lossos IS . Interleukin-4 distinctively modifies responses of germinal centre-like and activated B-cell-like diffuse large B-cell lymphomas to immuno-chemotherapy . *Br J Haematol* . 2009 ; Nov 147 : ( 3 ) 308 - 318
- 50 . Schmitter D , Koss M , Niederer E , Stahel RA , Pichert G . T-cell derived cytokines co-stimulate proliferation of CD40-activated germinal centre as well as follicular lymphoma cells . *Hematol Oncol* . 1997 ; Nov 15 : ( 4 ) 197 - 207
- 51 . Gocheva V , Wang HW , Gadea BB , Shree T , Hunter KE , Garfall AL . IL-4 induces cathepsin protease activity in tumor-associated macrophages to promote cancer growth and invasion . *Genes Dev* . 2010 ; Feb 1 24 : ( 3 ) 241 - 255



**Figure 1**

Phenotypic characterization of CD4<sup>pos</sup> T cells in malignant and reactive SLO

Frequency of CXCR5<sup>hi</sup>ICOS<sup>hi</sup> (A, B), CXCR5<sup>hi</sup>PD-1<sup>hi</sup> (B), and FOXP3<sup>pos</sup>CD25<sup>pos</sup> (C) among CD4<sup>pos</sup> T cells from tonsils (Tons), reactive LN (rLN), FL LN, and DLBCL LN samples. (A) Open squares represent rLN samples with a strong follicular hyperplasia. Bars: median. \* p<0.05; \*\*p<0.001; \*\*\*p<0.0001.

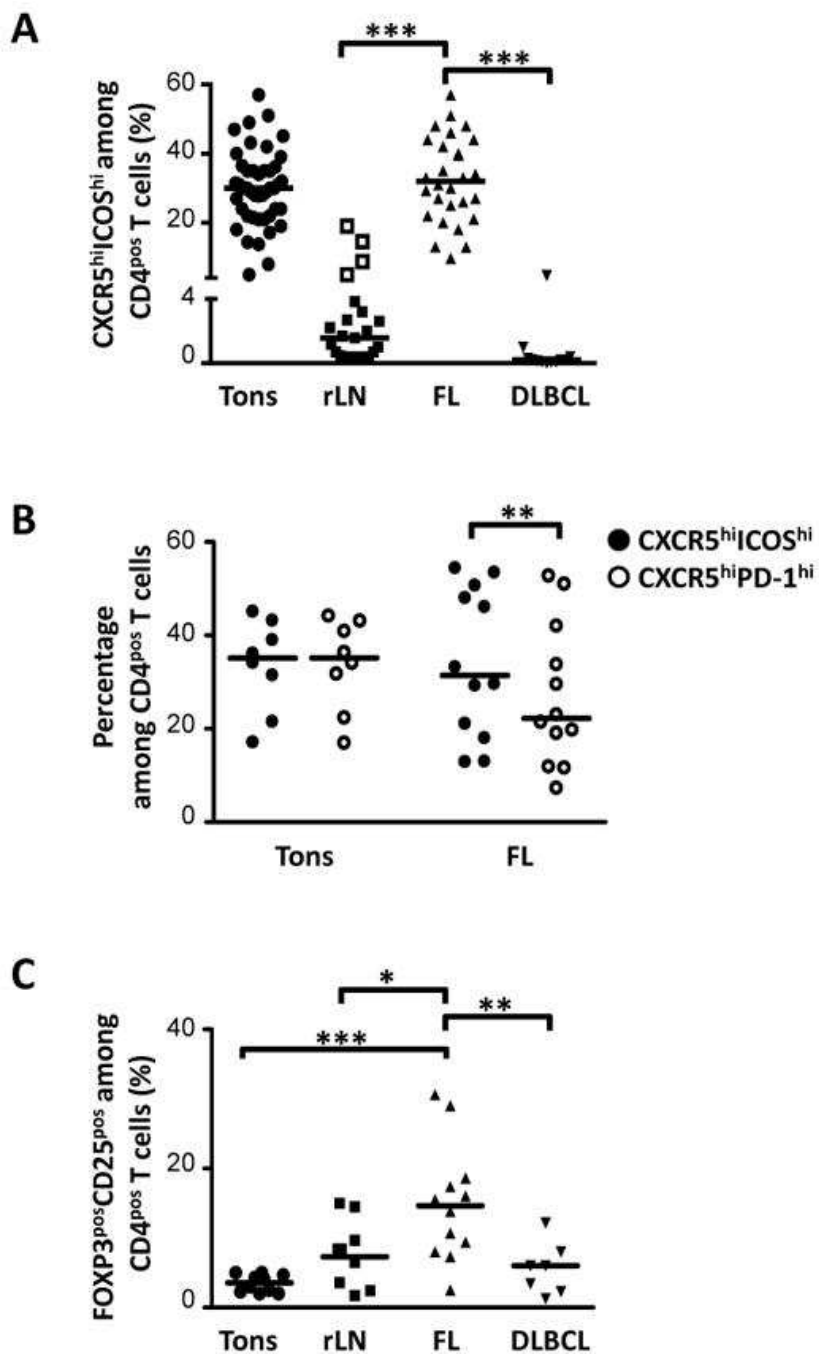


**Figure 2**

Phenotypic characterization of FL  $T_{FR}$

(A) *Left*: Representative plots of CD25 and FOXP3 expression among CXCR5<sup>hi</sup> ICOS<sup>hi</sup> CD4<sup>pos</sup> T cells in FL. *Right*: Frequency of CD25<sup>pos</sup> FOXP3<sup>pos</sup> subset among CD4<sup>pos</sup> CXCR5<sup>hi</sup> ICOS<sup>hi</sup> T cells from tonsils (Tons) and FL LN. (B) CXCR5 expression of CD25<sup>pos</sup> FOXP3<sup>pos</sup> cells among CD4<sup>pos</sup> T cells in Tons and FL LN. (C) Correlation between the percentage of  $T_{FR}$ , and the percentages of Treg or  $T_{FH}$  in FL LN.

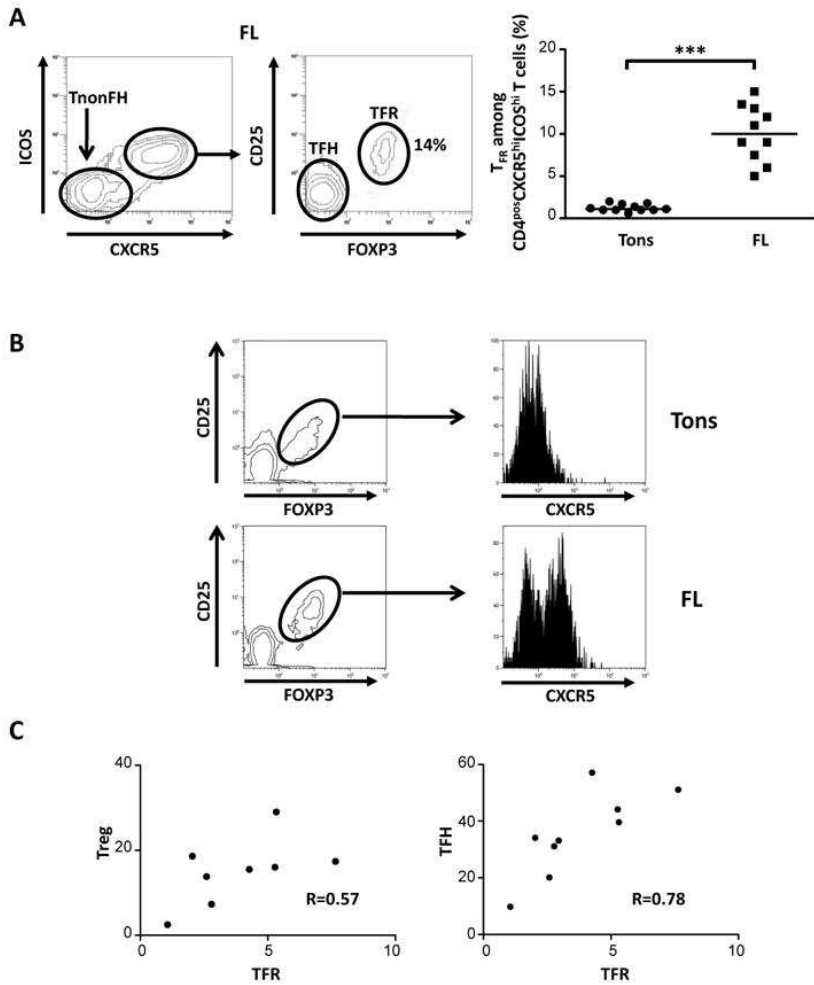


**Figure 3**

FOXP3<sup>pos</sup> ICOS<sup>pos</sup> cells in FL LN and reactive SLO

Immunohistochemistry in biopsies of (A) two cases of FL (1,2; respectively x100 and X400; 3,4; respectively X100 and X400), and (B) a reactive tonsil (1,2; respectively x100 and X250) and a LN with follicular hyperplasia (3,4; respectively X100 and X250). Double staining for FOXP3 (nuclear, blue) and ICOS (membrane, brown) show only very few cells expressing both markers in reactive tonsils and LN, mainly surrounding reactive GC (arrows) whereas a significant proportion of cells – either scattered or in small clusters - in the neoplastic follicles of FL are double stained for FOXP3 and ICOS.

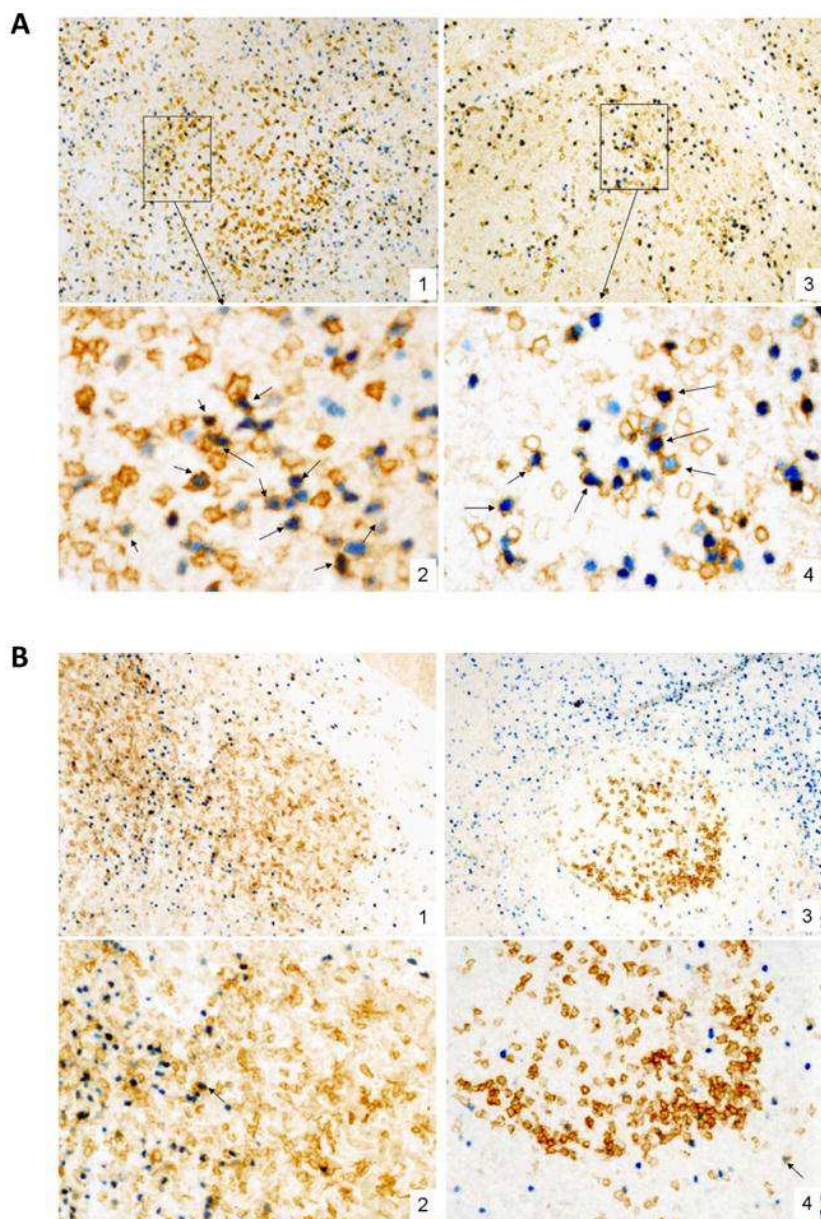


**Figure 4**

Gene expression of FL  $T_{FH}$  and  $T_{FR}$

(A) PCA of data resulting from the gene expression analyses of Th1, Th2, Th17, Treg, tonsil-derived  $T_{FH}$  (Tons), FL-derived  $T_{FR}$  and  $T_{FH}$ . (B) Hierarchical clustering of Treg, FL  $T_{FH}$  and  $T_{FR}$ , and Tons  $T_{FH}$ . (C) *TBX21*, *GATA3*, *RORC*, *FOXP3*, *BCL6*, *PRDM1*, and *PDCD1* gene expression in FL  $T_{FH}$  and  $T_{FR}$ , and Tons  $T_{FH}$  were compared to that in Th1, Th2, Th17 and Treg (n=4 for Tons  $T_{FH}$ , FL  $T_{FH}$  and  $T_{FR}$ , n=3 for Th1, Th2, Th17, and Treg). The arbitrary value of 1 was assigned to blood naive  $CD4^{pos}$  T cells. Bars: mean $\pm$ SD.

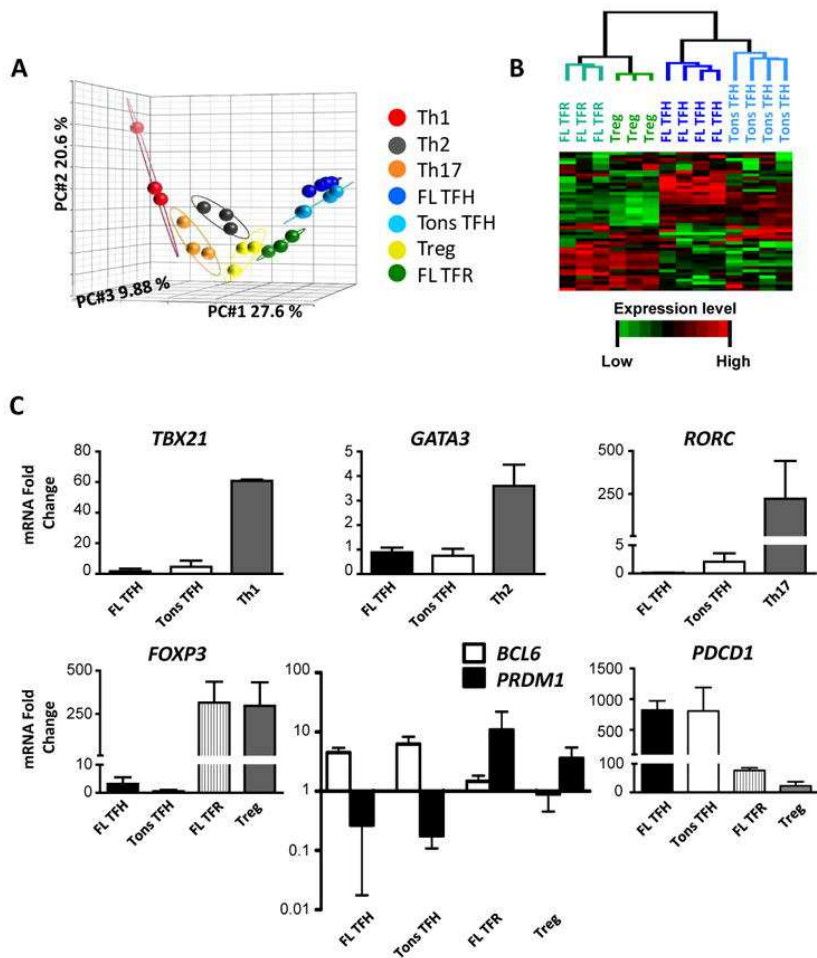


**Figure 5**

Functional characterization of FL  $T_{FH}$  and  $T_{FR}$

(A,B) Purified FL B cells were cultured alone or with autologous  $T_{FH}$ , non $T_{FH}$ , or  $T_{FR}$ . (A) *Left*: representative plots of CD86 (line) or isotype-matched (grey) staining on gated B cells. *Right*: CD86 expression fold change after coculture with  $T_{FH}$  or non $T_{FH}$ . The RMFI for each coculture condition was compared to the RMFI of B cells cultured alone, allowing the calculation of the ratio of RMFI (RRMFI). Bars: mean  $\pm$  SD (n=3). (B) *Left*: representative plots of active caspase-3 staining on gated B cells. *Right*: Percentages of inhibition of B-cell apoptosis in coculture with T subsets. Bars: mean  $\pm$  SD (n=3). (C) Activated (A) or non-activated (NA) CFSE-labelled effector T cells (Teff) were cultured alone or in presence of Teff, Treg, or  $T_{FR}$ ,  $T_{FH}$ , and non $T_{FH}$  isolated from FL LN. *Left*: representative plots of CFSE staining. *Right*: Bars: percentages of CFSE<sup>pos</sup> Teff displaying less (<G2, black) or more ( $\geq$ G2, white) than 2 cell divisions (n=3).

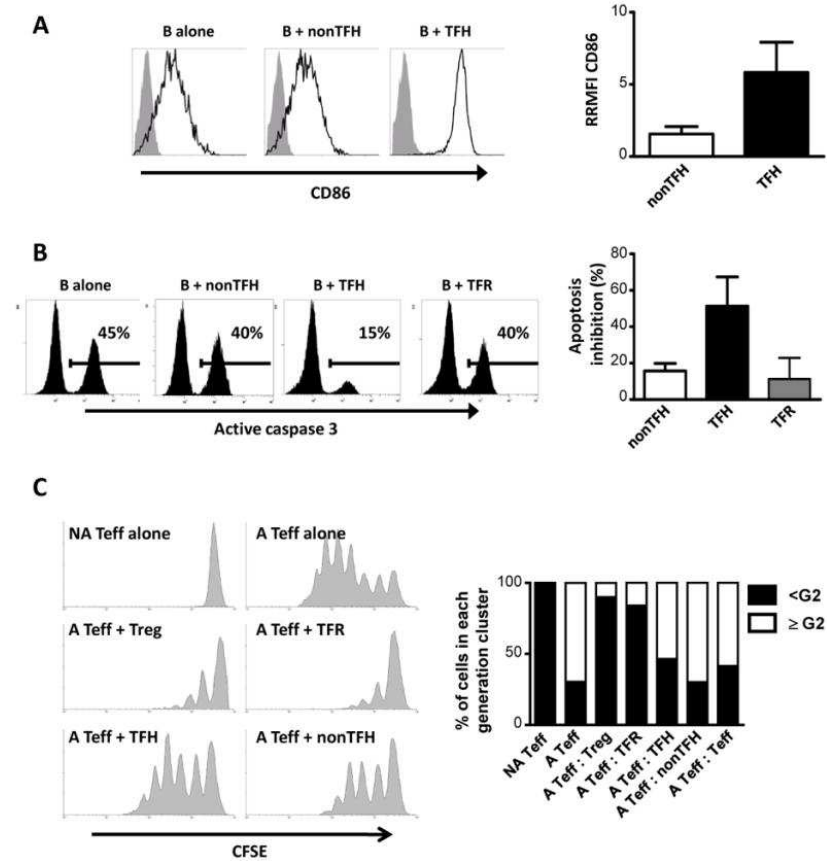


**Figure 6**

CD40L and IL-4 involvement in FL B-cell survival

(A) *IL4* and *CD40LG* expression of Tons and FL T<sub>FH</sub>. The arbitrary value of 1 was assigned to blood naive CD4<sup>pos</sup> T cells. Bars: mean±SD (n=6). \*p<0.05, \*\*p<0.01. (B,C) *Left*: representative plots of IFN-γ (B) or IL-4 (C) expression of activated (A) or non-activated (NA) PD1<sup>pos</sup> FL T<sub>FH</sub>. *Right*: expression of IFN-γ (•B) or IL-4 (C) by T<sub>FH</sub> or CD3<sup>pos</sup> T cells from Tons or FL LN. Bars: median. \*p<0.05, \*\*p<0.01. (D) Relative number of viable FL B cells after culture in presence or not of Rituximab and CD40L+/-IL-4. Number of viable FL B cells obtained without CD40L+IL-4 and without Rituximab was assigned to 100. Bars: median (n=9). \*\*p<0.01.

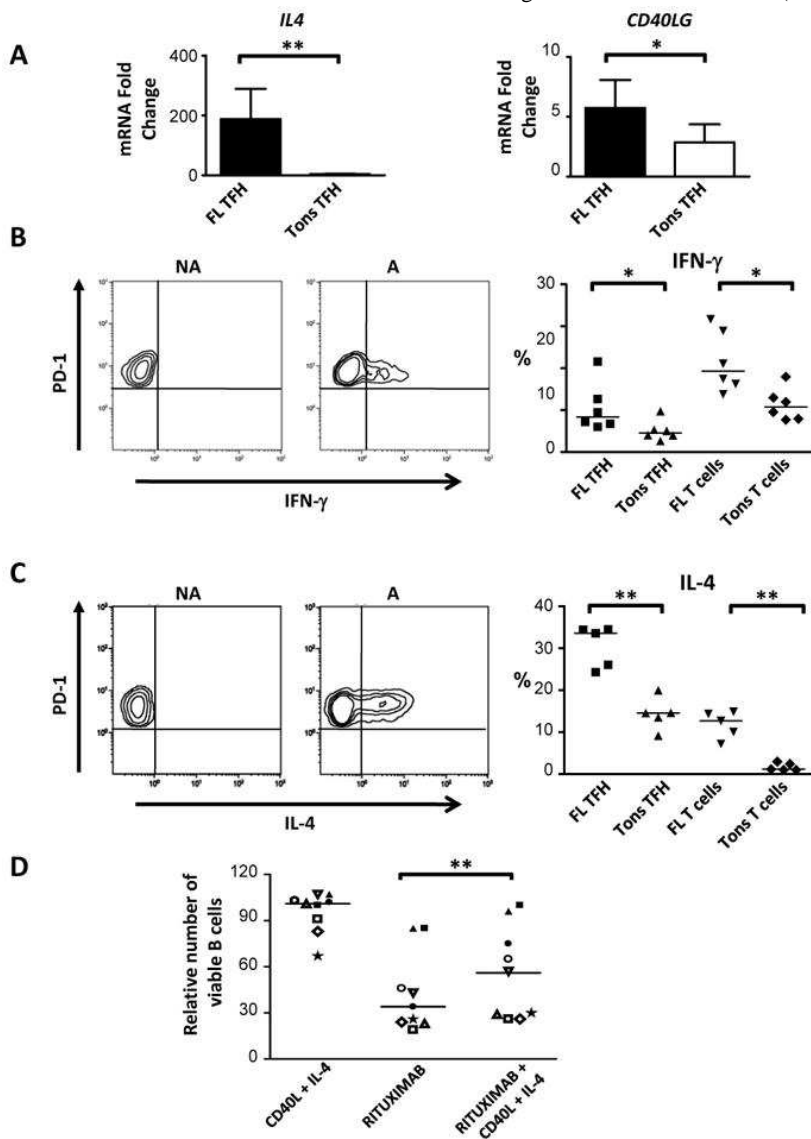


**Table 1**List of the 10 genes differentially expressed by sorted FL T<sub>FH</sub>, compared to tonsil (Tons) T<sub>FH</sub>.

Gene Symbol	Median of expression in FL T <sub>FH</sub>	Median of expression in Tons T <sub>FH</sub>	Ratio of median expression (FL T <sub>FH</sub> /Tons T <sub>FH</sub> )
<i>IL4</i>	<b>171.1</b>	<b>4.3</b>	<b>39.8</b>
<i>IL2</i>	76.4	3.4	22.3
<i>IFNG</i>	<b>10.1</b>	<b>1.8</b>	<b>5.5</b>
<i>TNF</i>	29.6	6.8	4.3
<i>CD200</i>	56.7	21.1	2.7
<i>CD40LG</i>	<b>6.5</b>	<b>2.5</b>	<b>2.6</b>
<i>AHR</i>	2.6	1.1	2.4
<i>LTA</i>	2.8	1.4	2.0
<i>RORC</i>	0.05	2.1	0.02
<i>IL26</i>	0.41	36.0	0.01